




Supplementary Material: Analyzing Data Augmentation Methods for Convolutional Neural Network-based Brain-Computer Interfaces

 **Gabriel Faria,***  **Gabriel Henrique de Souza,**  **Heder Bernardino,**
Luciana Motta, and  **Alex Vieira**
Federal University of Juiz de Fora
Juiz de Fora, Brazil

July 14, 2022

*The corresponding author can be contacted via gabriel.oliveira.moreira@ice.ufjf.br.

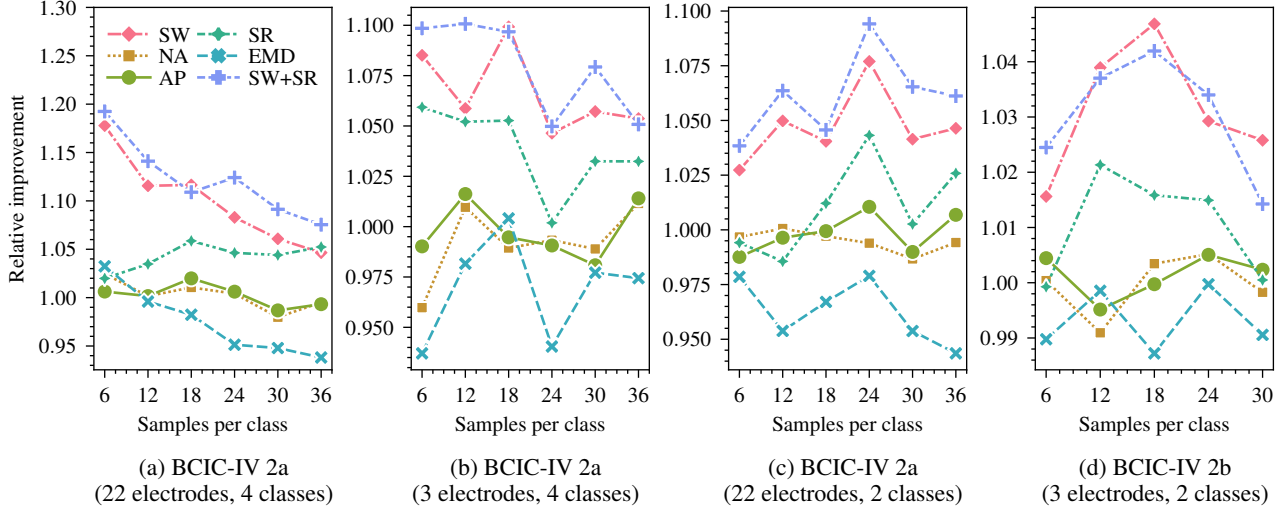


Figure 1: Mean test accuracy improvement (relative to the baseline) for within-session 4-fold cross-validation with respect to the number of original training samples per class, averaged over subjects, sessions, and folds. SW is Sliding Window, NA is Noise Addition, AP is Amplitude Perturbation, SR is Segmentation and Recombination, and EMD is Empirical Mode Decomposition.

Table 1: Mean test accuracies (\pm standard deviation) for within-session 4-fold cross-validation.

| Method # Samples | Baseline | SW | NA | AP | SR | EMD | SW+SR |
|--|-------------------|-------------------------------------|-------------------|-------------------|-------------------|-------------------|-------------------------------------|
| (a) BCIC-IV 2a (22 electrodes, 4 classes) | | | | | | | |
| 6 | 0.369 \pm 0.134 | 0.434 \pm 0.172 | 0.378 \pm 0.140 | 0.371 \pm 0.132 | 0.376 \pm 0.144 | 0.381 \pm 0.130 | 0.440 \pm 0.181 |
| 12 | 0.477 \pm 0.170 | 0.532 \pm 0.179 | 0.478 \pm 0.177 | 0.478 \pm 0.174 | 0.494 \pm 0.186 | 0.475 \pm 0.164 | 0.545 \pm 0.181 |
| 18 | 0.513 \pm 0.193 | 0.573 \pm 0.181 | 0.519 \pm 0.201 | 0.524 \pm 0.195 | 0.543 \pm 0.186 | 0.504 \pm 0.169 | 0.569 \pm 0.192 |
| 24 | 0.563 \pm 0.185 | 0.609 \pm 0.177 | 0.565 \pm 0.193 | 0.566 \pm 0.187 | 0.589 \pm 0.205 | 0.535 \pm 0.182 | 0.633 \pm 0.183 |
| 30 | 0.600 \pm 0.189 | 0.636 \pm 0.178 | 0.588 \pm 0.187 | 0.592 \pm 0.188 | 0.626 \pm 0.184 | 0.569 \pm 0.183 | 0.655 \pm 0.173 |
| 36 | 0.627 \pm 0.187 | 0.656 \pm 0.179 | 0.623 \pm 0.181 | 0.622 \pm 0.190 | 0.659 \pm 0.181 | 0.588 \pm 0.179 | 0.674 \pm 0.185 |
| (b) BCIC-IV 2a (3 electrodes, 4 classes) | | | | | | | |
| 6 | 0.374 \pm 0.126 | 0.406 \pm 0.139 | 0.359 \pm 0.126 | 0.370 \pm 0.124 | 0.396 \pm 0.130 | 0.351 \pm 0.123 | 0.411 \pm 0.157 |
| 12 | 0.441 \pm 0.135 | 0.466 \pm 0.139 | 0.445 \pm 0.139 | 0.448 \pm 0.141 | 0.464 \pm 0.155 | 0.432 \pm 0.142 | 0.485 \pm 0.145 |
| 18 | 0.472 \pm 0.154 | 0.519 \pm 0.135 | 0.467 \pm 0.155 | 0.470 \pm 0.151 | 0.497 \pm 0.154 | 0.474 \pm 0.143 | 0.518 \pm 0.136 |
| 24 | 0.515 \pm 0.144 | 0.539 \pm 0.116 | 0.512 \pm 0.152 | 0.510 \pm 0.141 | 0.516 \pm 0.135 | 0.485 \pm 0.147 | 0.541 \pm 0.117 |
| 30 | 0.523 \pm 0.130 | 0.553 \pm 0.119 | 0.517 \pm 0.134 | 0.513 \pm 0.131 | 0.540 \pm 0.129 | 0.511 \pm 0.121 | 0.564 \pm 0.129 |
| 36 | 0.535 \pm 0.128 | 0.564 \pm 0.123 | 0.542 \pm 0.129 | 0.543 \pm 0.125 | 0.553 \pm 0.123 | 0.522 \pm 0.132 | 0.563 \pm 0.118 |
| (c) BCIC-IV 2a (22 electrodes, 2 classes) | | | | | | | |
| 6 | 0.593 \pm 0.153 | 0.609 \pm 0.155 | 0.591 \pm 0.153 | 0.586 \pm 0.148 | 0.590 \pm 0.158 | 0.580 \pm 0.157 | 0.616 \pm 0.173 |
| 12 | 0.643 \pm 0.170 | 0.675 \pm 0.186 | 0.644 \pm 0.178 | 0.641 \pm 0.177 | 0.634 \pm 0.178 | 0.613 \pm 0.173 | 0.684 \pm 0.183 |
| 18 | 0.667 \pm 0.175 | 0.694 \pm 0.195 | 0.666 \pm 0.179 | 0.667 \pm 0.183 | 0.676 \pm 0.193 | 0.645 \pm 0.190 | 0.698 \pm 0.193 |
| 24 | 0.697 \pm 0.181 | 0.750 \pm 0.181 | 0.693 \pm 0.186 | 0.704 \pm 0.182 | 0.727 \pm 0.180 | 0.682 \pm 0.192 | 0.762 \pm 0.175 |
| 30 | 0.726 \pm 0.185 | 0.756 \pm 0.171 | 0.716 \pm 0.182 | 0.719 \pm 0.190 | 0.728 \pm 0.182 | 0.693 \pm 0.200 | 0.774 \pm 0.178 |
| 36 | 0.731 \pm 0.176 | 0.765 \pm 0.175 | 0.727 \pm 0.177 | 0.736 \pm 0.181 | 0.750 \pm 0.184 | 0.690 \pm 0.189 | 0.776 \pm 0.175 |
| (d) BCIC-IV 2b (3 electrodes, 2 classes) | | | | | | | |
| 6 | 0.643 \pm 0.167 | 0.653 \pm 0.170 | 0.643 \pm 0.168 | 0.646 \pm 0.166 | 0.643 \pm 0.169 | 0.637 \pm 0.168 | 0.659 \pm 0.172 |
| 12 | 0.667 \pm 0.174 | 0.693 \pm 0.179 | 0.661 \pm 0.177 | 0.663 \pm 0.173 | 0.681 \pm 0.179 | 0.666 \pm 0.174 | 0.691 \pm 0.182 |
| 18 | 0.686 \pm 0.187 | 0.718 \pm 0.183 | 0.688 \pm 0.187 | 0.686 \pm 0.189 | 0.697 \pm 0.184 | 0.677 \pm 0.188 | 0.714 \pm 0.190 |
| 24 | 0.704 \pm 0.184 | 0.725 \pm 0.175 | 0.708 \pm 0.187 | 0.708 \pm 0.186 | 0.715 \pm 0.187 | 0.704 \pm 0.182 | 0.728 \pm 0.180 |
| 30 | 0.720 \pm 0.178 | 0.738 \pm 0.173 | 0.718 \pm 0.179 | 0.721 \pm 0.177 | 0.720 \pm 0.185 | 0.713 \pm 0.183 | 0.730 \pm 0.182 |

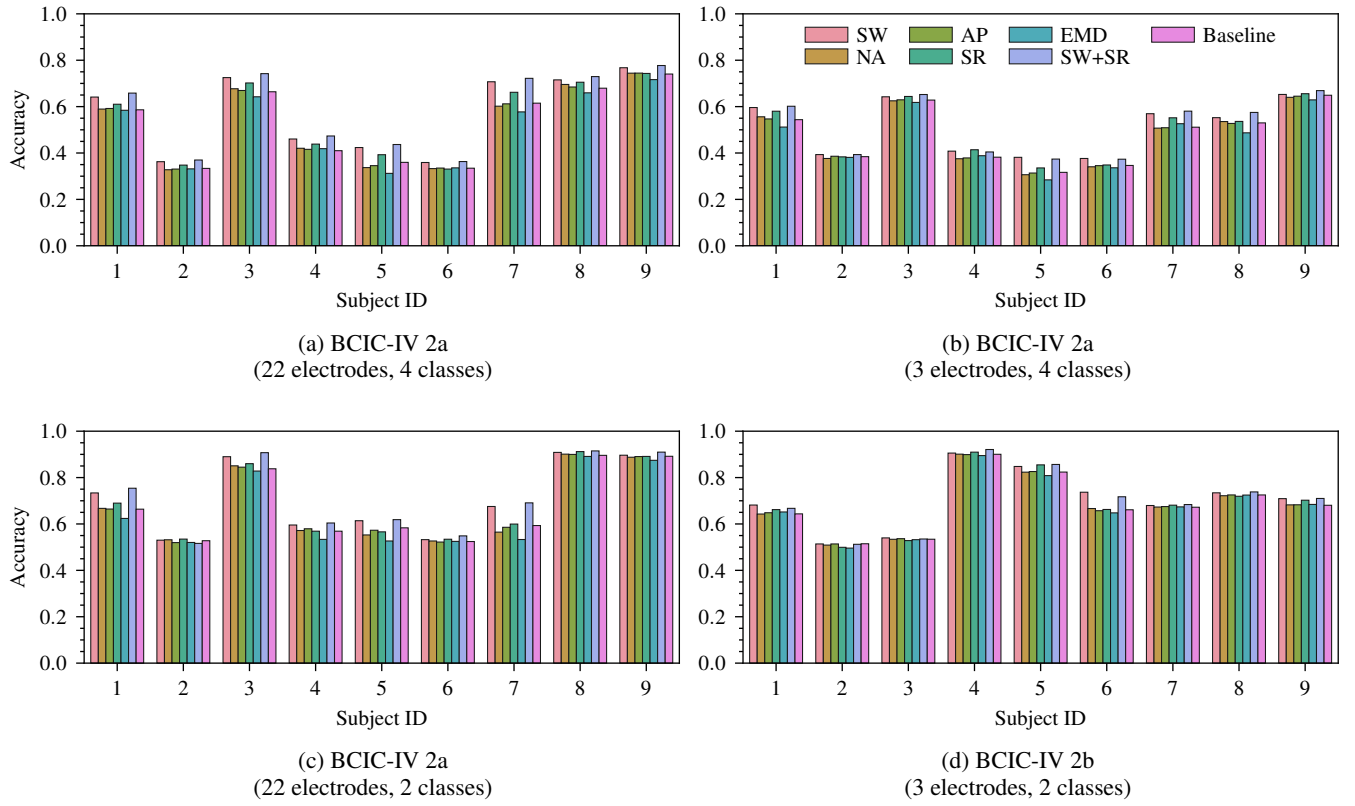


Figure 2: Subject-wise mean test accuracy for within-session 4-fold cross-validation.

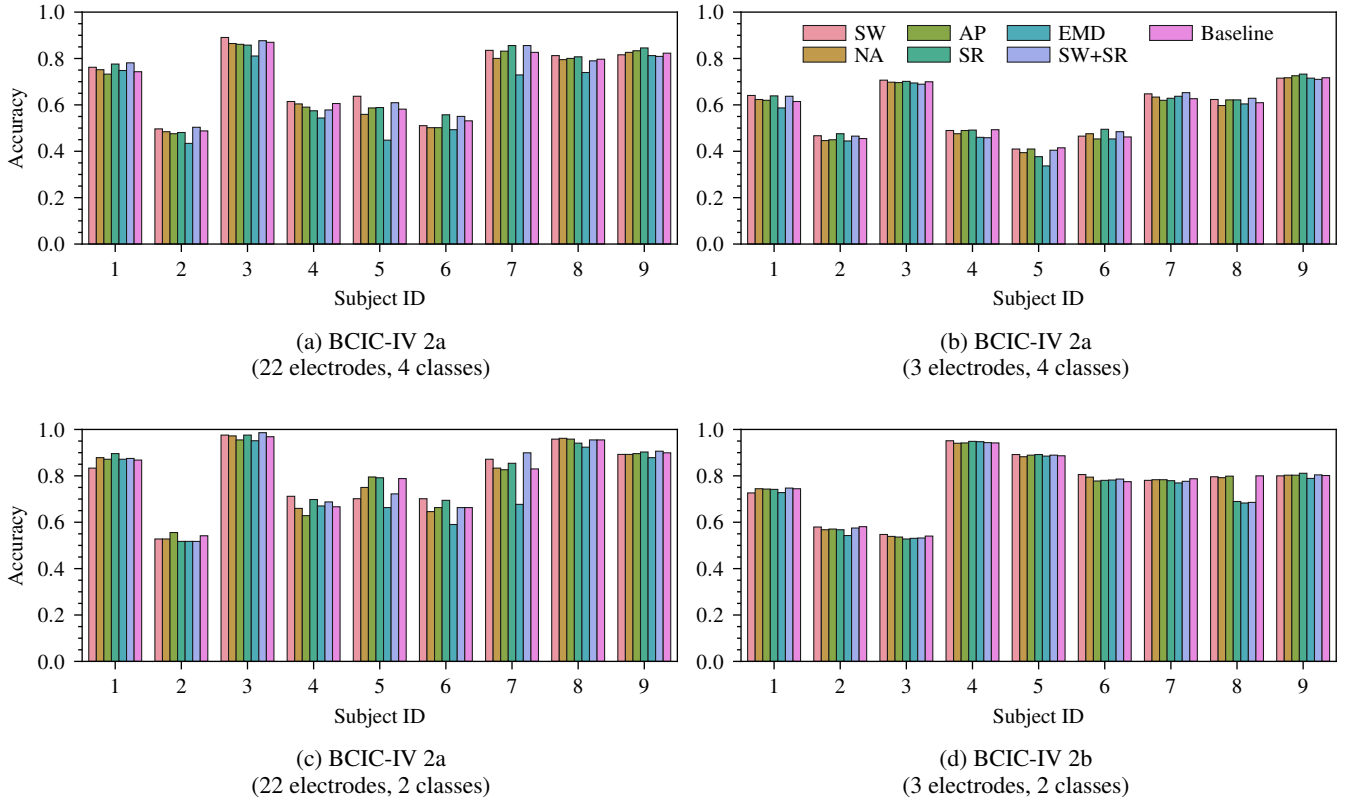


Figure 3: Subject-wise mean test accuracy for cross-session 4-fold cross-validation.

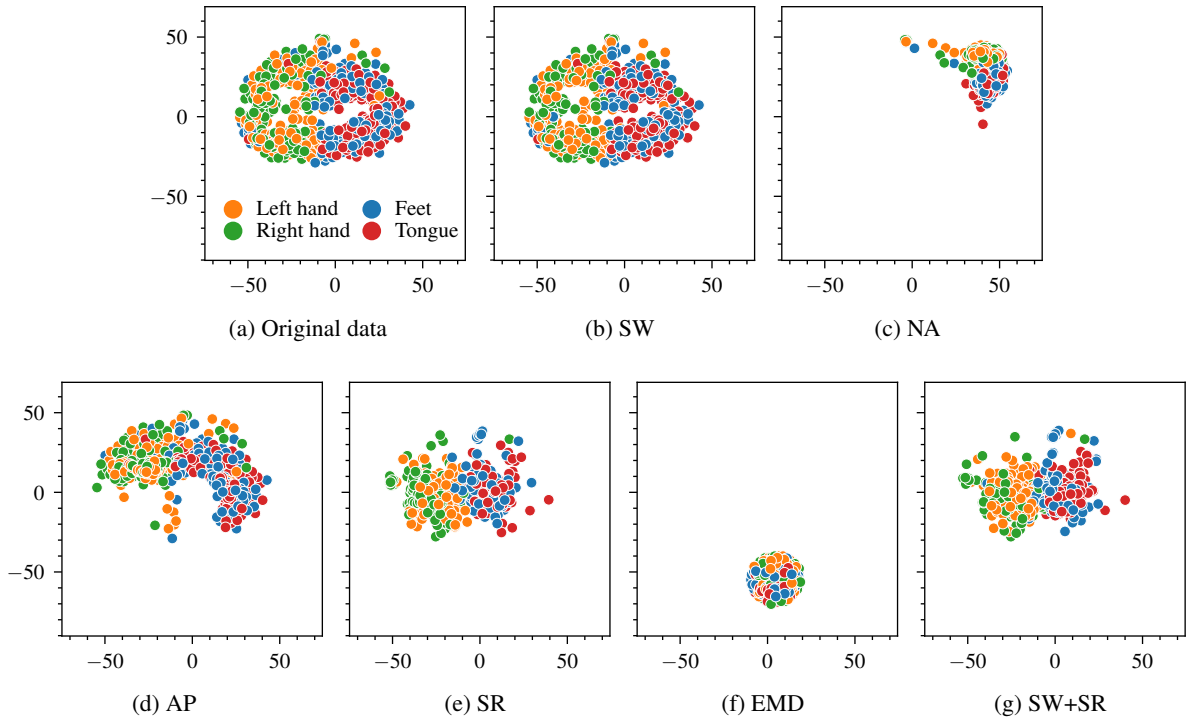


Figure 4: Two-dimensional t-SNE projections of the covariance matrices of the signals from subject 1 of dataset BCIC-IV 2a using the Riemannian distance. The signals were not band-pass filtered.

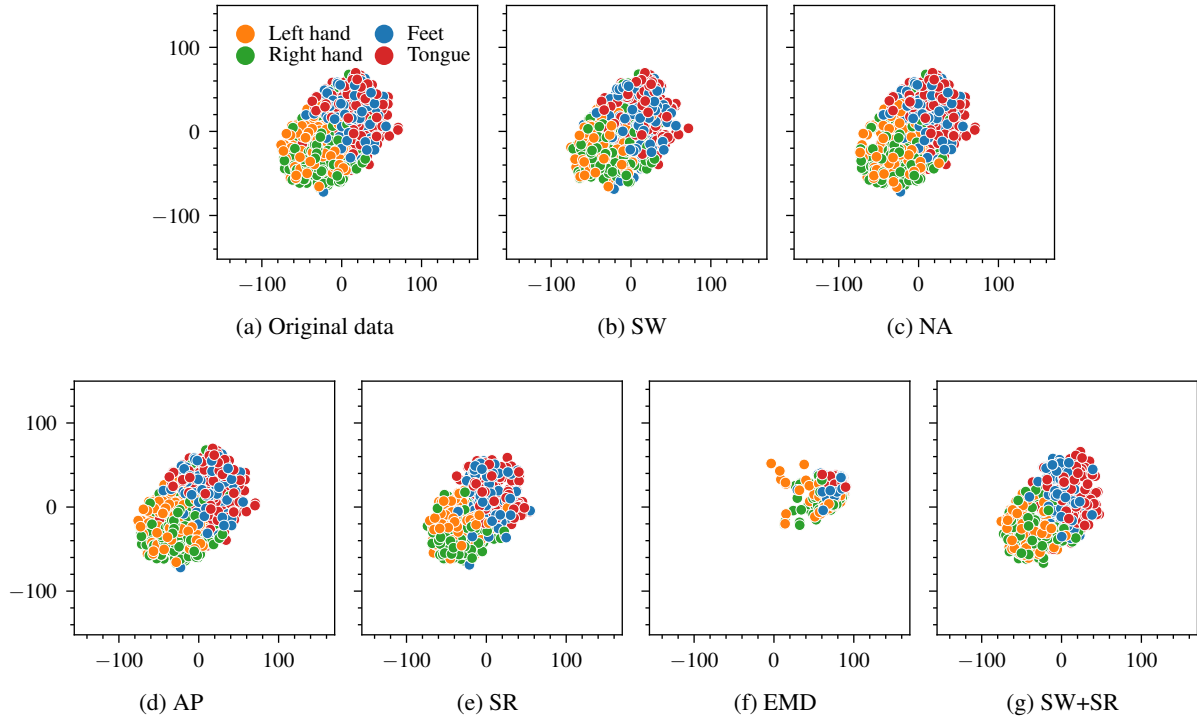


Figure 5: Two-dimensional t-SNE projections of the covariance matrices of the signals from subject 1 of dataset BCIC-IV 2a using the Riemannian distance. Only the C3, Cz, and C4 electrodes were considered.

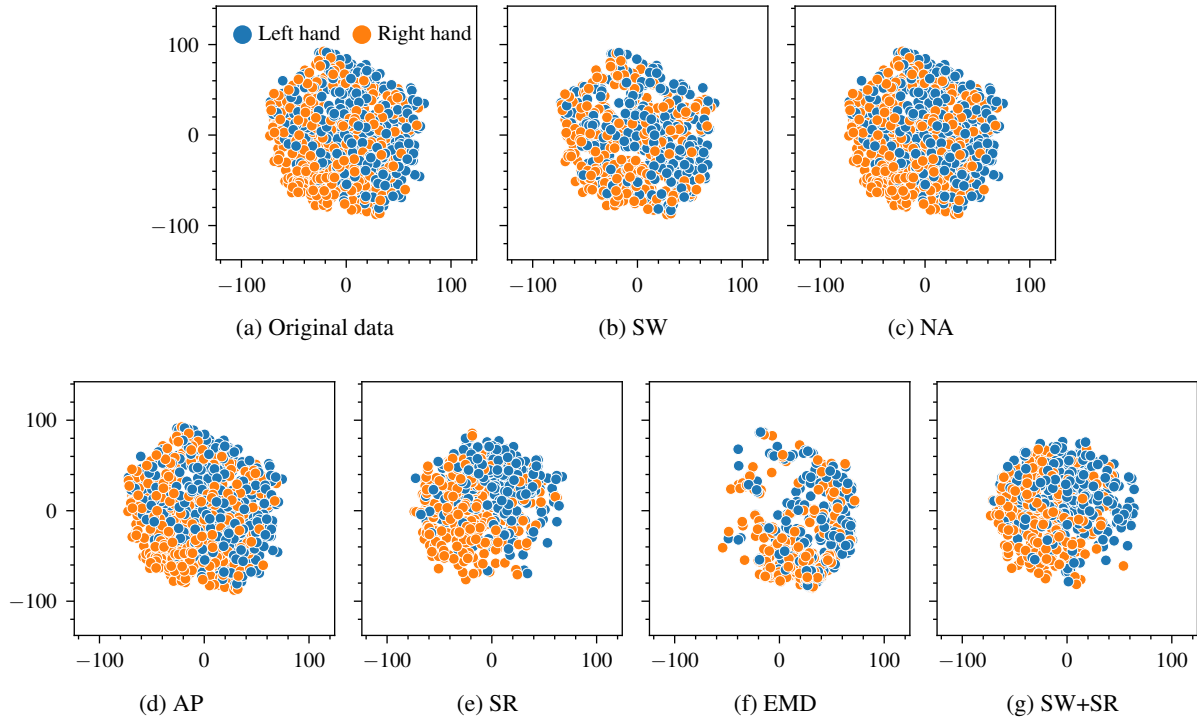


Figure 6: Two-dimensional t-SNE projections of the covariance matrices of the signals from subject 1 of dataset BCIC-IV 2b using the Riemannian distance.

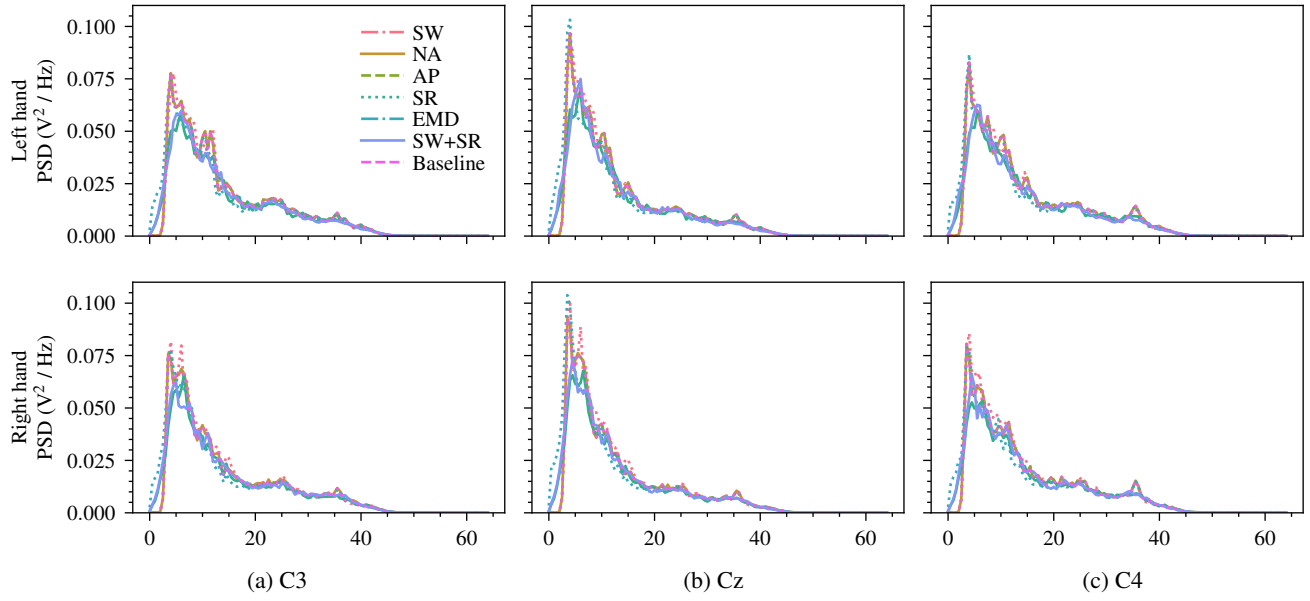


Figure 7: Mean power spectral density of the C3, Cz, and C4 electrodes for left and right-hand motor imagery signals from subject 1 of the BCIC-IV 2a dataset.

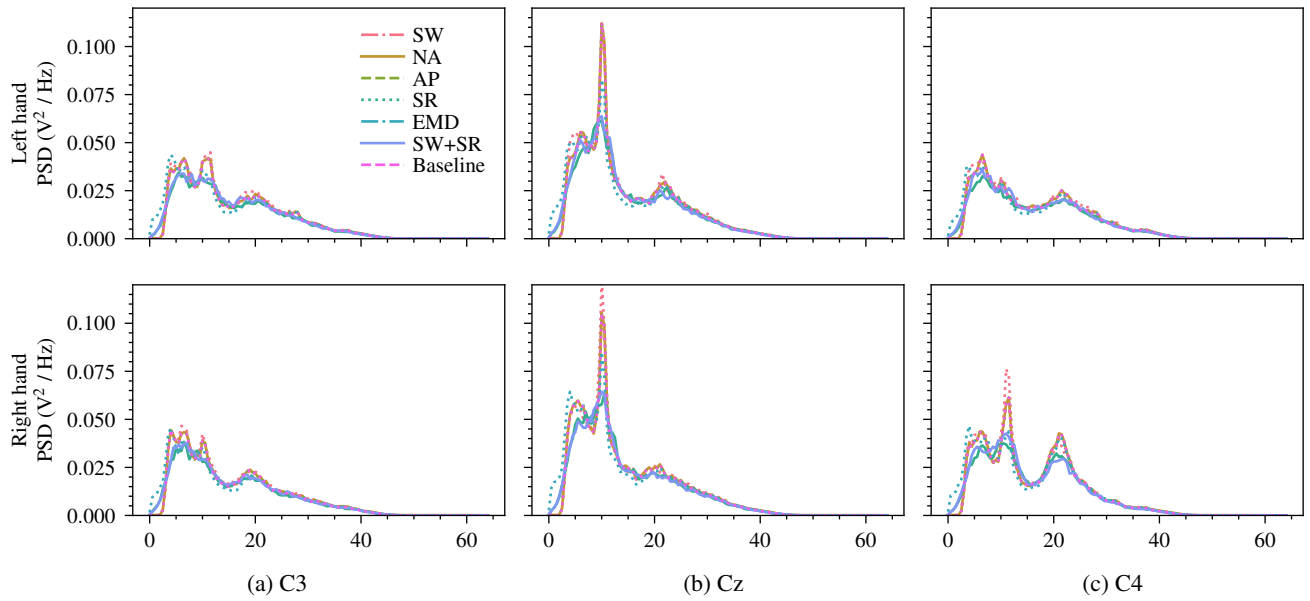


Figure 8: Mean power spectral density of the C3, Cz, and C4 electrodes for left and right-hand motor imagery signals from subject 1 of the BCIC-IV 2b dataset.

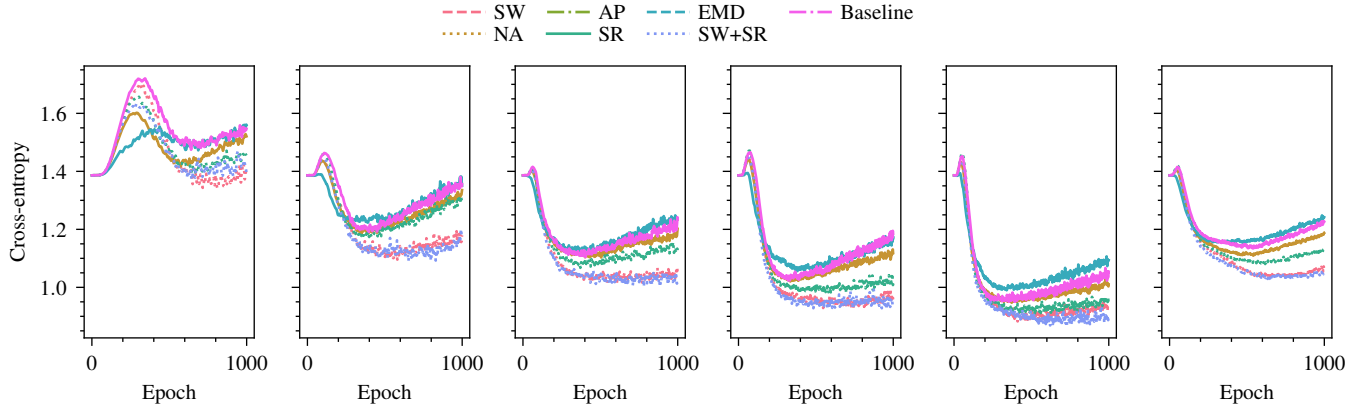


Figure 9: Mean validation loss in the within-session scenario on the BCIC-IV 2a dataset (22 electrodes and 4 classes). From left to right, each plot corresponds to the following amount of training samples per class: 6, 12, 18, 24, 30, and 36.

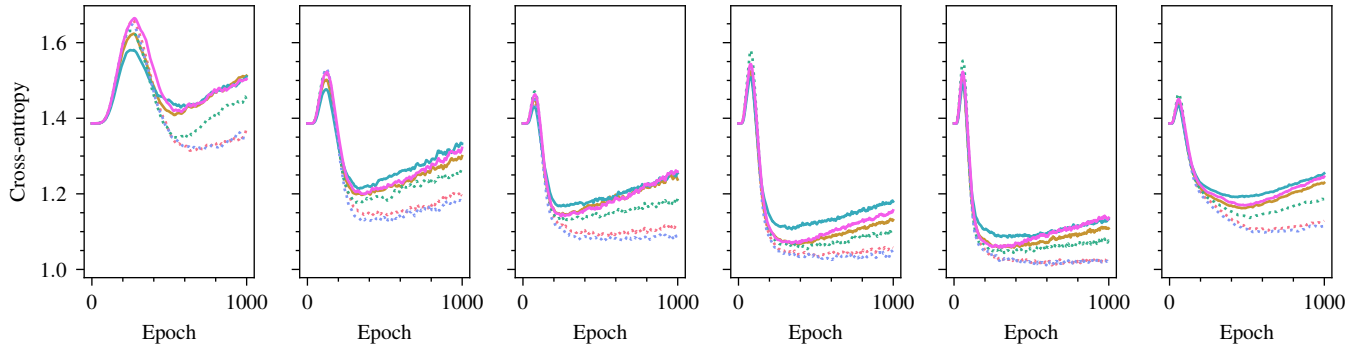


Figure 10: Mean validation loss in the within-session scenario on the BCIC-IV 2a dataset (3 electrodes, 4 classes). From left to right, each plot corresponds to the following amount of training samples per class: 6, 12, 18, 24, 30, and 36.

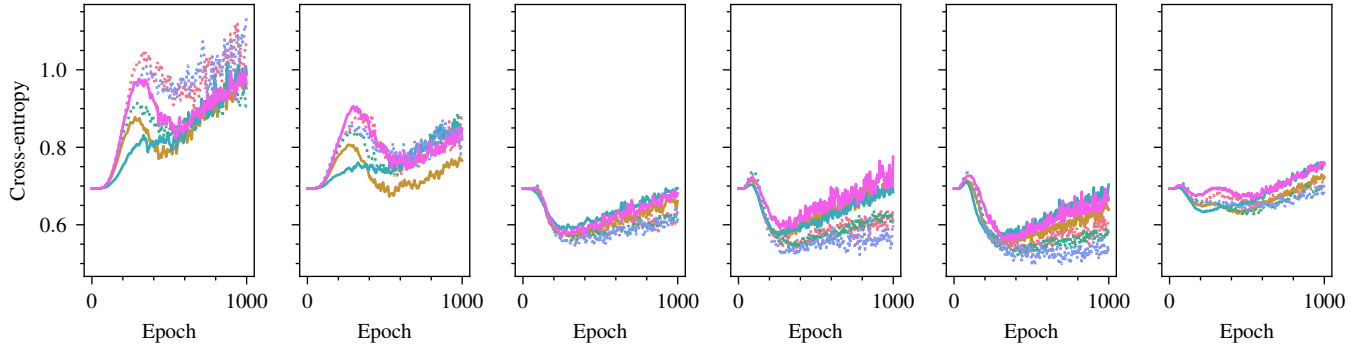


Figure 11: Mean validation loss in the within-session scenario on the BCIC-IV 2a dataset (22 electrodes, 2 classes). From left to right, each plot corresponds to the following amount of training samples per class: 6, 12, 18, 24, 30, and 36.

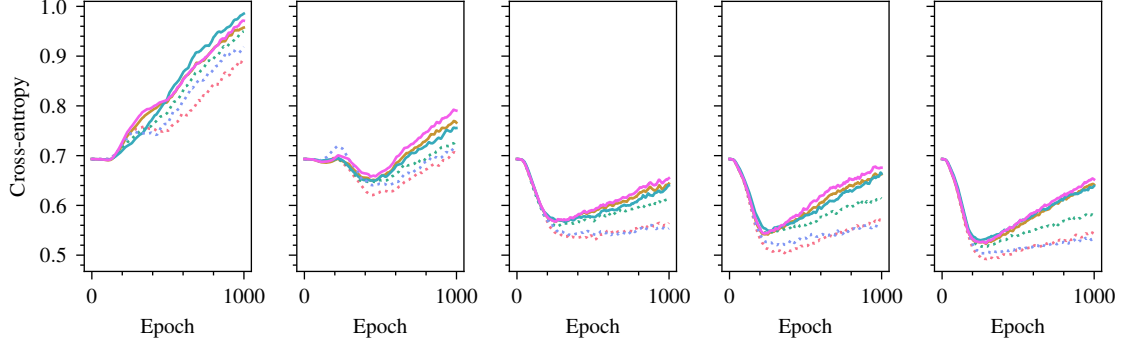


Figure 12: Mean validation loss curves in the within-session scenario on the BCIC-IV 2b dataset (3 electrodes, 2 classes). From left to right, each plot corresponds to the following amount of training samples per class: 6, 12, 18, 24, and 30.

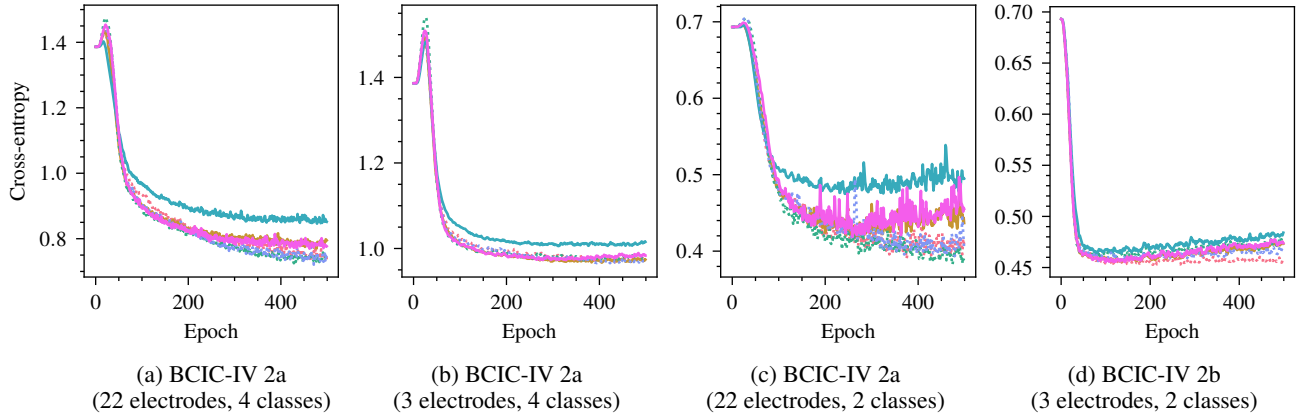


Figure 13: Mean validation loss curves in the cross-session scenario.